University of Baghdad
College of Engineering
JOURNAL OF ENGINEERING

Journal of Engineering

journal homepage: www.joe.uobaghdad.edu.iq

Volume 28 Number 12 December 2022

Chemical, Petroleum, and Environmental Engineering

Wormholes Models for the Optimum Matrix Acidizing in Mi4 Unit-Ahdeb Oil Field

Usama Sahib Alameedy *
PhD
College of Engineering-University of Baghdad
Baghdad-Iraq
E-mail: usama.sahib@coeng.uobaghdad.edu.iq

Ayad A.Alhaleem A.Alrazzaq
Prof. Dr.
College of Engineering-University of Baghdad
Baghdad-Iraq
E-mail: Dr.Ayad.A.H@coeng.uobaghdad.edu.iq

ABSTRACT

Innovative laboratory research and fluid breakthroughs have improved carbonate matrix stimulation technology in the recent decade. Since oil and gas wells are stimulated often to increase output and maximum recovery, this has resulted in matrix acidizing is a less costly alternative to hydraulic fracturing; therefore, it is widely employed because of its low cost and the fact that it may restore damaged wells to their previous productivity and give extra production capacity. Limestone acidizing in the Mishrif reservoir has never been investigated; hence research revealed fresh insights into this process. Many reports have stated that the Ahdeb oil field's Mishrif reservoir has been unable to be stimulated due to high injection pressures, which make it difficult to inject acid into the reservoir formation; and (ii) only a few acid jobs have been successful in Ahdeb oil wells, while the bulk of the others has been unsuccessful. Based on an acid efficiency curve, an ideal gel acid (HCl 15%) injection rate for this reservoir was 2.16 cc/min. This injection rate produces an optimal wormhole and the least amount of acid utilized. The optimum pore volume to breakthrough in wormhole propagation was 2.73, and the optimal interstitial velocity in wormhole propagation was 0.6 cm/min.

Researchers have developed new formulae to compute the skin factor in anisotropic carbonates generated from matrix acidizing for the first time. This experiment revealed the need to acidify the matrix at the optimal injection rate.

Keywords: Mishrif reservoir, skin factor, global wormhole propagation model, matrix acidizing.

موديلات الثقب الدودي لمعالجة الحشو الصخري الأمثل في الوحدة الرابعة لمكمن مشرف– حقل الاحدب

*Corresponding author
Peer review under the responsibility of University of Baghdad.
https://doi.org/10.31026/j.eng.2022.12.03

Article received: 4/6/2022
Article accepted: 4/7/2022
Article published: 1/12/2022

أسامة صاحب العميدي مدرس كلية الهندسة–جامعة بغداد	اياد عبد الحليم عبد الرزاق استاذ كلية الهندسة–جامعة بغداد

الخلاصة

أدت الأبحاث المختبرية المبتكرة واختراقات السوائل إلى تحسين تقنية تحفيز حشو الصخور الكربونية في العقد الأخير. ومع ذلك ، فإن الاستراتيجيات الحالية لتحسين تحفيز مكامن الكربونات غير فعالة. نظرًا لأن آبار النفط والغاز يتم تحفيزها في كثير من الأحيان لزيادة الإنتاج والاسترداد الأقصى ، فقد أدى ذلك إلى أن تكون عملية تحمض الحشو بديلاً أقل تكلفة للتكسير الهيدروليكي ؛ لذلك ، يتم توظيفها على نطاق واسع بسبب تكلفتها المنخفضة وحقيقة أنها قد تعيد الآبار المتضررة إلى إنتاجيتها السابقة وتوفر طاقة إنتاجية إضافية. لم يتم التحقق من تحميض الحجر الجيري في مكمن مشرف؛ ومن هنا كشف بحثنا عن رؤى جديدة في هذه العملية. ذكرت العديد من التقارير أن مكمن مشرف في حقل الاحدب النفطي لم يتم تحفيزه بسبب ضغوط الحقن العالية ، مما يجعل من الصعب حقن الحمض في تكوين الخزان ؛ و (2) لم ينجح سوى عدد قليل من الأعمال الحمضية في آبار النفط في الاحدب ، بينما لم ينجح الجزء الأكبر من الآبار الأخرى. بناءً على منحنى الكفاءة الحمضية ، كان معدل حقن حامض الهيدروكلوريك (تركيز 15%) المثالي لهذا الخزان 2.16 سم مكعب / دقيقة. ينتج معدل الحقن هذا ثقبًا دوديًا مثاليًا وأقل كمية من الحمض المستخدم. تبلغ قيمة PV (bt-optim) 2.73 و v (i-optim) = 0.6 سم / دقيقة. تتضمن أحدث نتائج هذه الدراسة نموذجًا عالميًا محسنًا لانتشار الثقوب ومعادلات جديدة لحساب عامل الجلد بسبب تحمض المصفوفة في الكربونات متباينة الخواص. سلطت نتائج هذه الدراسة الضوء على الحاجة إلى تحمض المصفوفة بمعدل الحقن المناسب.

الكلمات الرئيسية: مكمن مشرف, عامل الجلد, موديل الثقب الدودي, تحمض المصفوفة

1. INTRODUCTION

In the early 1980s, the Ahdeb oil field was discovered in Wasit province, **Fig. 1**. The 2D seismic acquisition for the contract area took place in 1977. Nine exploratory wells have been drilled and analyzed systematically in the oil-bearing region. Eight of them were showing a flow of oil. The deepest well was Ad-1, which reached Ratawi formation at a depth of 4057.0m, Lower Cretaceous**(Al-Waha Pet. Corp. Ltd., 2010; Azeez et al., 2020; Neeamy** and **Selman, 2020; Noori et al., 2019)**. In the middle of the Cretaceous Section, five pay zones were discovered. These pay zones are Khasib-2, Mishrif-4, Rumaila-1, Mauddud-1, and Rumaila-2b. For this study, after getting authorization for just a 1.5-meter section from the Mi4 unit of the Mishrif formation in well Ad-12, an oil-producing well, 11 plug samples from this section were recovered. The logging data from the Ahdeb field and the final well report, geological report, and stimulation report from the same formation are collected.

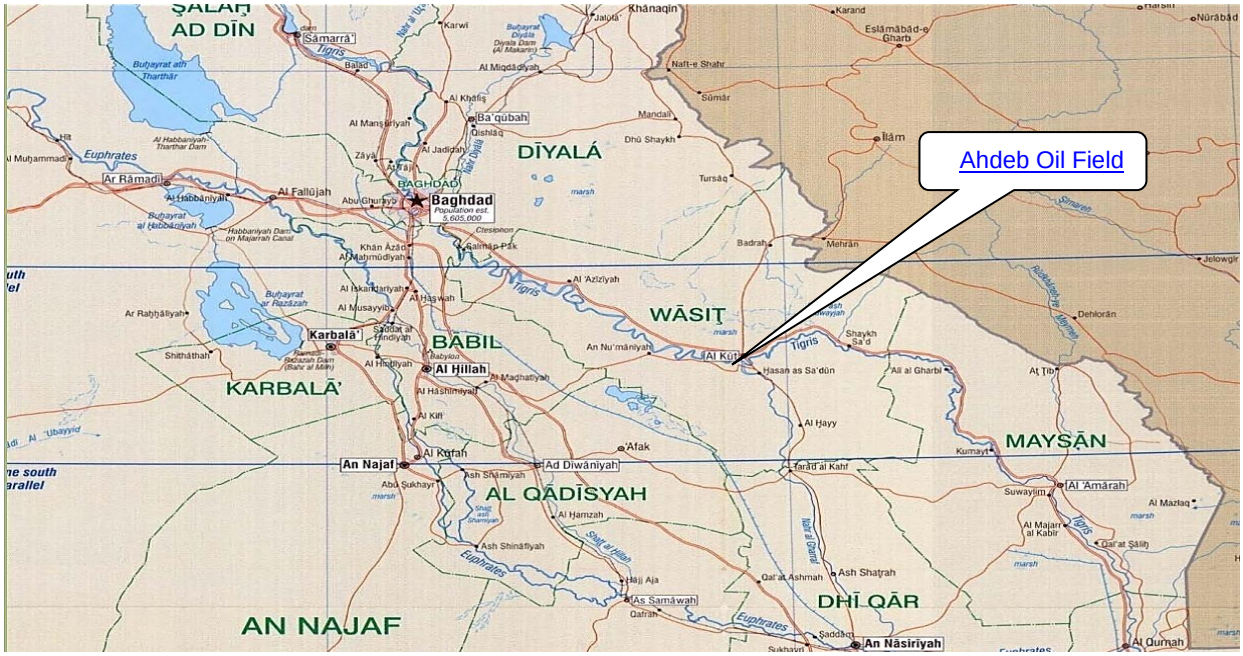

Figure Error! No text of specified style in document.. Ahdeb Field Location Map **(Al-Waha Pet. Corp. Ltd., 2010)**.

The Mishrif carbonate series stratigraphic structure is depicted in **Fig. 2**. Mishrif formation rocks can be divided into the following groups based on rock lithology and facies **(Al-Hashmi et al., 2010):**

- In contrast to reservoir rocks, compact limestone does not contain hydrocarbons that may be recovered. The porosity of this limestone ranges from 0 to 8.01%, and it is impermeable.
- Despite its low permeability, chalk limestone possesses tiny grains and high porosity (about 20 percent) (1.5 md). Fine clay-impregnated grains, moderate porosity (17%), and poor permeability characterize Lagoon Limestone (3.7 md).
- Reef limestone is divided into fine and intermediate grains and coarse and intermediate grains. It has a high porosity (23%) and excellent permeability(75md).
-

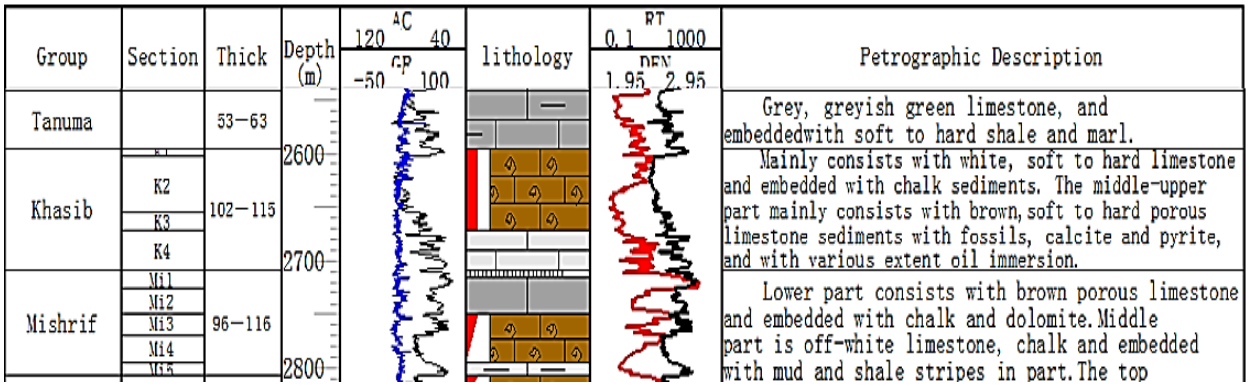

Figure 2. Mishrif carbonate series stratigraphic structure **(Al-Waha Pet. Corp. Ltd., 2010)**

Numerous scholars have studied wormhole formation during carbonate acidification to understand the process better and predict the optimal parameters for obtaining the best outcomes. Possibly devised by **(Schechter and Gidley, 1969)**, an earlier model may have taken into account changes in particle size due to reactivity on the pore's surface. According to **(Daccord** and **Lenormand, 1987),** wormholes propagate in accordance with the fractal dimension of $d_f \approx 1.6$, which is consistent with this discovery. This model has the drawback of being great at interstitial velocities over the optimum need while failing at small, suboptimal velocities. The inefficient and poor wormhole propagation is not taken into account. In reality, it does not anticipate an ideal condition and predicts that $r_{wh} \rightarrow \infty$ as q Approaches 0.

(Daccord et al., 1989) developed an entirely new model, which used the fractal structure of this process to establish an exact quantitative correlation between the ideal acidifying conditions. The wormholed area has no pressure decrease because the wormholes are deemed endlessly conducive compared to the original reservoir. Daccord et al. demonstrated via radial propagation experiments that those wormholes form a fractal structure having fractal dimension $df \approx 1.6$. Radius rises with increasing time, as shown by the formula, $r_{wh} \propto t^{\alpha}$, where $\propto\approx 0.7$ for 2D (thin) radial structures and with 3D radial structures, the latter having a time constant of $\propto\approx 0.65$. This translates into a significant fact on wormhole propagation: in these studies, the value of PV_{bt} dropped as the wormholes spread farther from the center. This would be the case if PV_{bt} was constant, as the injected acid volume is directly proportional to the wormholed volume. As $\sqrt{t}$ increases, r_{wh} rises, resulting in an α value of 0.5 in this scenario. When it comes to fact, the wormhole spreading is more efficient as the wormholes develop; in other words, the effective PV_{bt} decreases as r_{wh} grows. Since well performance is affected by matrix acidizing treatment, estimating the wormholed area is necessary. Hill invented and published the volumetric model **(Economides et al., 1994).** It assumes a constant pore volume at breakthrough (PV_{bt}), which is a highly useful and simple model. It's easy to predict the length of the wormhole using only one variable, PV_{bt}. In order to assure accuracy, it's best to use an average PV_{bt} value or a constant interstitial velocity during stimulation. The near-wellbore flow is radial; therefore, the interstitial velocity decreases as acid goes away from the wellbore. For example, the value of PV_{bt} is affected by injection time, which is not considered in volumetric flow models.

(Fredd and **Fogler, 1996)** demonstrated that the various dissolving patterns correlate to certain Damköhler number ranges. Damköhler numbers of about 0.29 have been associated with the best injection rate for all rocks, acids, and chelating agents. The Damköhler number is the ratio of the net reaction rate to the acid transport rate by convection. The dissolving rate may be controlled by the reaction rate or diffusion of acid or reaction products in materials with slow reaction rates, such as limestone, weak acids, and dolomites. When the dissolution rate (including diffusion phases and reaction) contradicts the acid convection rate, Damköhler's number helps to understand why this is so. Slow injection velocity (high Damköhler number) results in face dissolving because the acid reacts before it is supplied by convection. Convection removes the acid before it can react with the mineral, resulting in wormholes or a uniform disintegration when the injection velocities

are too high (low Damköhler number). A narrow wormhole is formed in the rock when diffusion, reaction rates, and convection are balanced at the ideal Damköhler number. Despite its intriguing theoretical implications, the presence of an ideal Damköhler number is difficult to implement in acidizing process design due to a large number of unknown factors (pore diameters and mass transfer coefficients) involved in its computation.

(Gong and **El-Rabaa, 1999)**'s model for radial wormhole propagation incorporates the fractal dimension introduced by **(Daccord** and **Lenormand, 1987)** but uses a mix of dimensionless numbers to describe both the optimum and inefficient wormhole propagation at lower flow rates. Even more impressive, it was used by **(McDuff et al., 2010)** to match results from testing on large slabs of carbonate rocks, the largest wormhole trials yet recorded. To be clear, the length calculated here does not have length dimensions but rather one with a dimension equal to the square root of $(2/d_f)$ of a length unit. Wormhole propagation requires $d_f \approx 1.6$, not 2; hence this is not a length dimension; this leads to incorrect calculations when used in practice, which is a theoretical contradiction. Calculating injection time to achieve a certain wormhole length using this method, for example, provides a different result when different length units are used. **(Huang et al., 1999)** proposed an alternative representation of the Damköhler number**. (Mahmoud et al., 2011)** introduced a Péclet number-based model. Using statistical analysis of pore sizes, **(Dong et al., 2017)** came up with a new model for the wormhole extension. **(Fredd** and **Fogler, 1996)** provided in-depth analyses of wormhole models. These models were divided by the latter into seven categories:

- Péclet number models.
- Damköhler number models.
- Capillary tube models.
- Transition pore theory models.
- Averaged continuum (or two-scale) models.
- Network models.
- Semi-empirical models.
-

2. Research Methodology and Mathematical Models

Typically, the optimal matrix acidizing conditions may be determined by a series of flooding experiments in the laboratory **(Alameedy et al., 2022)**. Since each point on the curve necessitates a full-scale experiment of core flooding, this is a time-consuming and costly procedure **(Alameedy, 2022)**.

2.1 Wormhole Propagation Global Models

Theoretical approaches to wormhole propagation modeling exist; however, they are difficult to apply in the actual field. Therefore, the presumed global models are often utilized for field-size treatment planning. Wormhole propagation rates may be predicted using macroscopic semi-empirical models based on data collected around a wellbore **(Economides et al., 2013).**

There is an empirical correlation that may fit the acid efficiency curve of PV_{bt} vs. v_i,, using just the coordinates of the optimum point $PV_{bt,opt}$ and $v_{i,opt}$ as inputs. **(Buijse** and **Glasbergen, 2005)**. When it comes to matching experimental data, its looks have a strong association. It has also been proposed that the correlation in the radial geometry may be leveraged by calculating the interstitial velocity as an average at the front of the wormholed zone **(Buijse** and **Glasbergen, 2005).**

$PV_{bt,opt}$ and $v_{i,opt}$ are the only parameters required by this model. Experimental results show that this curve takes on the same shape when interstitial velocities are either too high or not precise enough. By integrating the velocity over time, the radius of the wormholed region may then be determined.

The model developed by Buijse and G lasbergen served as the basis for Tar dy's innovative notion of self-diverting acids. A continual increase in the model's PV_{bt} was also provided as an alternative to Buijse and Glasberge n's model. A similar technique to that given by Bui jse **(Tardy et al., 2007)** is used for upscaling from linear and core flow to field size and radial flow: v_i, is determined as the average at the front of the wormhole. Other elements like acid content, temperature, and core aspect ratio were considered by **(Talbot** and **Gdanski, 2008)** while developing a new model based on Bujse's. These researchers proposed a method for transforming data acquired at one temperature and acid concentration into another using the variables $PV_{bt,opt}$ and $v_{i,opt}$. The plug length is divided by the cross-sectional area to determine the model's aspect ratio. There is no way to cope with this aspect ratio when scaling up from core and linear flow to field size and radial flow. Wellbore scale calculations are carried out using the $PV_{bt,opt}$ and $v_{i,opt}$ values acquired in core flooding tests in Buijse's model and its adaptations. Even the core scale measurements, as previously indicated, alter dramatically when the diameter of the core varies. Hence, it should be predicted that values of $PV_{bt,opt}$ and $v_{i,opt}$ typical for the full wellbore will differ from those recorded using cores.

The reported values of $PV_{bt,opt}$ and $v_{i,opt}$ are strongly reliant on the diameter of the cores employed to measure them; hence, the influence of core size is an essential but sometimes overlooked element of wormholing research.

According to **(Economides et al., 2013)**, three global models are the most often used: **(Buijse** and **Glasbergen, 2005)**'s model, Economides' volumetric model, and **(Furui et al., 2012c)**'s model. In addition to **(Daccord et al., 1989)**, **(Tardy et al., 2007),** and **(Talbot** and **Gdanski, 2008)**, many more global models may be used for comparison.

2.1.1 The Volumetric Model

The simplest method assumes that a certain percentage of the rock punctured will dissolve in the acid to figure out how much acid is required to move wormholes a certain distance. This notion, known as the volumetric model, was first introduced by **(Economides et al., 1994)**.

As a few wormholes are constructed, only a small percentage of the rock is dissolved; as more branching wormhole structures are developed, a bigger matrix fraction is dissolved. The radius at which a wormhole may propagate is

$$r_{wh} = \sqrt{r_w^2 + \frac{V}{PV_{bt}\pi\phi h}} \quad (1)$$

The PV_{bt} is the only wormhole propagation parameter needed for this concept in equation 3.8, which may be obtainable from core-flood experiments.

2.1.2 The Buijse-Glasbergen Model

The empirical model of wormhole propagation proposed by **(Buijse** and **Glasbergen, 2005)** is based on the typical dependency of the PV_{bt} in acid core floods on the interstitial velocity. There is a constant functional relationship between wormhole propagation velocity and the PV_{bt} for various rocks and different acid systems. They came up with a function to represent this reliance based on this premise. Using the Buijse and Glasbergen model, it can be can say

$$v_{wh} = \frac{d_{r_w}}{d_t} = \left(\frac{v_i}{PV_{bt-opt}}\right)\left(\frac{v_i}{v_{i-opt}}\right)^{-y}\left\{1 - exp\left\langle -4\left(\frac{v_i}{v_{i-opt}}\right)^2\right\rangle\right\}^2 \quad (2)$$

By simply stating the ideal condition, the minimum pore volumes to breakthrough $(PV_{bt-\mathrm{opt}})$ value and the optimal interstitial velocity $v_{i-\mathrm{opt}}$ value; therefore, the $PV_{bt-\mathrm{opt}}$–$v_{i-\mathrm{opt}}$ relationship may be conveniently established. A single calibration point is required to fit this model to a specific acid-rock system.

The wormhole velocity is determined by the $v_{i-\mathrm{opt}}$ at the wormhole front, r_{wh}, and decreases as the wormhole area front advances away from the wellbore.

2.1.3 The Furui et al. Model

(Furui et al., 2012b) developed a novel semi-empirical model based on **(Buijse and Glasbergen 2005)**, but with a unique upscaling technique to represent the wellbore size. As wormholes grow, the values of $PV_{bt,opt}$ and $v_{i,opt}$ at the field, scale vary from those found at the core size in this model, and they do not remain constant. An adjustment was made when calculating interstitial velocity using a region's outer area average. By looking at how much higher the interstitial velocity at wormhole tips than at the average $\bar{v}_i$ is, and by performing tests and numerical simulations to verify this, they concluded that the wormhole propagation velocity is driven by the higher than average interstitial velocity $v_{i,tip}$ of dominant wormholes.

$$v_{wh} = v_{i,\,ip}\, N_{Ac} \times \left(\frac{v_{i,\,ip}}{v_{i,\,tip,opt}}\right)^{-\gamma} \times \left\{1 - exp\left[-4\left(\frac{v_{i,\,ip}}{v_{i,\,ip\,,\,opt}}\right)^2\right]\right\}^2 \quad (3)$$

(Furui et al., 2012a) extended their work and published equations for $v_{i,opt}$ for the spherical and radial wormholes propagation. When using a radial flow field, the first is most suited for acidizing open-hole or highly perforated wells. The equation was modified to assume spherical flow from each hole rather than a restricted entrance method with a small number of perforation holes to make it more suitable for acid injection from remote locations. This model predicts a larger wormholing velocity by linking it with the interstitial tip velocity and guesses a slower falling rate

of that velocity. Furui et al. models predict that for radial wormhole propagation, for example, $v_{i,opt}$ decreases proportionally to $\frac{1}{\sqrt{r_{wh}}}$ for $\alpha_z = 0$ or does not decline at all (for $\alpha_z = 1$), whereas the Buijse-Glasbergen model estimates that $\bar{v}_i$ rises proportionally to $1/\sqrt{r_{wh}}$.

These models were utilized by **(Furui et al., 2012a** and **Furui et al., 2012b)** and shown to be more accurate with field data than the Buijse-Glasbergen model using $PV_{bt,opt}$ and $v_{i,opt}$ measurements obtained in a laboratory. It does, however, include other changeable factors, such as α_z , mwh and dewh, which have been found to be difficult to predict. Eventually, these factors should also be historically matched.

A fascinating model (Furui et al., 2010) considers the results collected at various scales and has been effectively used to match field data. But there are a few drawbacks: (1) it requires input parameters such as wormhole cluster diameter and wormhole count that are difficult to measure or estimate; (2) the predicted field results can change when data from different core sizes are used as input; and (3) it does not reverse back to the Buijse and Glasbergen correlation when representing core scale.

2.1.4 Schwalbert Model

(Schwalbert et al., 2017) improved **(Buijse** and **Glasbergen, 2005)**'s model by including scaling factors $f_1$and f_2 that adjust $v_{i,opt,\,\text{core}}$ and $PV_{bt,opt,core}$ to the field size. In this new suggested global wormhole model, interstitial acid velocity $\bar{v}_i$ is linked to the wormhole front's propagation velocity, v_{wh} by:

$$v_{wh} = \frac{\bar{v}_i}{PV_{bt,opt,core} \times f_1} \left(\frac{\bar{v}_i}{v_{i,opt,\,core} \times f_2} \right)^{-1/3} \left\{ 1 - exp \left[-4 \left(\frac{\bar{v}_i}{v_{i,opt,\,core} \times f_2} \right)^2 \right] \right\}^2 \quad (4)$$

The scaling factors$f_1$and f_2 can be calculated as follows:

$$f_1 = \left(\frac{d_{core}}{d_{s1}} \right)^{\varepsilon_1} \quad (5)$$

$$f_2 = \left(\frac{d_{\text{core}}}{d_{s2}} \right)^{\varepsilon_2} \quad (6)$$

d_{s1} and d_{s2} are typical scales for wormhole propagation. $PV_{bt,opt,core}$ and $v_{i,opt,core}$ are widespread to yield the values predicted at any other scale diameter d:

$$PV_{bt,opt}(d) = PV_{bt,opt,core} \left(\frac{d_{core}}{min(d, d_{rep,1})} \right)^{\varepsilon_1} \quad (7)$$

$$v_{i,opt}(d) = v_{i,opt,core} \left(\frac{d_{core}}{min(d, d_{rep,2})} \right)^{\varepsilon_2} \quad (8)$$

Observe that if ε_1=ε_2 =0, this model reduces back to **(Buijse** and **Glasbergen, 2005)**'s if the interstitial velocity is estimated as the average at the front of wormholes, which is represented by $\bar{v}_i$. Flow's geometrical characteristics are influenced by $\bar{v}_i, v_{wh}, d_{s1}$ and d_{s2}.

2.1.4.1 Divergence and heterogeneous rock types.

The majority of carbonate rocks are heterogeneous and exhibit large permeability differences, complicating implementing treatments of matrix acidizing **(Pereira et al., 2012)**. **Fig. 3** by (**Al-Yaseri et al., 2013; Alameedy, 2012)** provides an example of a carbonate reservoir with a high-contrast permeability distribution. The wormholes in the more permeable zones become longer, while those in the less permeable zones get shorter.

Fluid placement or diversion procedures are the approaches to cope with this challenge and boost the acid penetration in the limited permeability zones **(Economides et al., 2013)**. Heterogeneous distribution of wormhole penetration may be achieved even using fluid implantation procedures, which must be considered when calculating the skin factor.

Various models may estimate the amount of acid injected into the multiple zones. Two basic methods are used in these simulations: discretizing the neighboring reservoir and the wellbore into separate segments, each with its permeability, and then computing the acid injection rate into each section over time. **(Furui et al., 2012b)** provided an example of a model tailored exclusively for carbonates. **(Doerler** and **Prouvost, 1987; Hill** and **Galloway, 1984; Taha et al., 1989)** are models that apply various diverting agents.

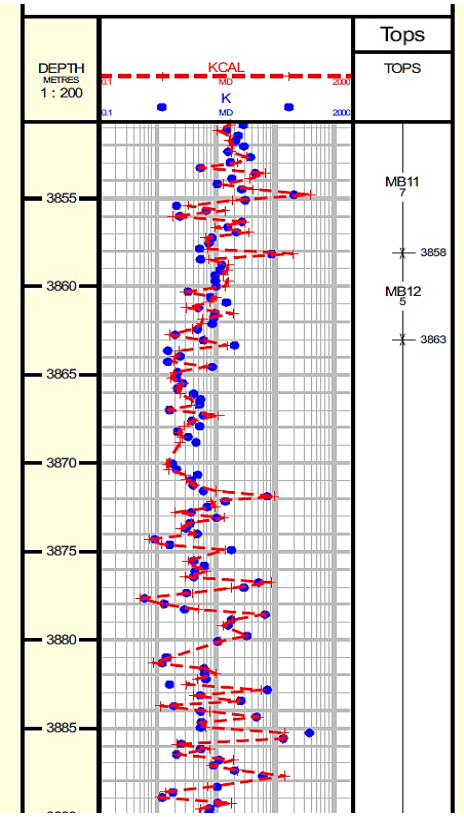

Figure 3. Permeability profile in a carbonate reservoir **(Al-Yaseri et al., 2013)**.

According to these hypotheses, the length of the wormhole varies because of variations in the quantity of acid injected into each section. Each section's skin factor is computed using the Hawkins method, and the total skin factor is as well. The skin factor for a vertical well may be

added using **Eq. 9**, which provides the total skin factor. Researchers **(Furui et al., 2003)** developed a mathematical formula for estimating a horizontal well's overall "skin" factor using an analytical equation.

$$s_{eq} = \frac{\int_0^L k(z)dz}{\int_0^L \left[\frac{k(z)}{\ln\left(\frac{r_e}{r_w}\right)+s(z)}\right]dz} - \ln\left(\frac{r_e}{r_w}\right) \quad (9)$$

Where s_{eq} is the equivalent overall skin factor, r_e is the drainage area external radius of the well, and L is the length of the horizontal well.

2.1.4.2 Propagation of Wormhole in Anisotropic Rocks.

According to **(Bagrintseva, 2015)**, carbonate reservoirs may be divided into two categories: those with highly anisotropic rocks (complex reservoir rocks) and those that are slightly isotropic (pore-type reservoirs). Natural fractures, layering, or vugs on various scales contribute to the anisotropy of permeability in complex-type reservoirs.

The permeability of these reservoirs may vary by order of magnitude depending on the flow direction **(Bagrintseva, 2015).** Vertical permeability is typically lower than horizontal permeability **(Lucia, 2007)**, although natural fissures may increase vertical permeability **(Widarsono et al., 2006).** In order to match expected and historical performance, the vertical permeability sometimes has to be 100 times lower than the horizontal permeability **(Lucia, 2007)**. There is no wormhole model for anisotropic formations, and there is no discussion of the geometry of the stimulated zone, according to what the author knows. Anisotropic carbonate wormhole distribution has been overlooked in the scientific literature. An elliptical damage distribution has traditionally been assumed to occur in horizontal wells in anisotropic rocks when addressing damage distribution; this assumption was first presented by (**Furui et al., 2003)**, when acidifying, the wormhole distribution isn't provided.

2.2 Monitoring the performance of acidizing treatment (Economides et al., 2013)

Analyzing the injection rate and pressure during injection is recommended for monitoring a matrix acidizing treatment in a carbonate reservoir, in the same way as monitoring a sandstone acidizing treatment is advised. In carbonates, the pressure loss across the wormhole zone is assumed to be insignificant, which means that the wormhole impact on the wellbore skin effect is equivalent to extending the wellbore. The skin's evolution after a carbonate matrix acidizing treatment may be anticipated using wormhole propagation models under this assumption.

As the wormhole penetration radius increases in a damaged well with a permeability *k*, the skin effect is proportional to the wormhole penetration radius as follows:

$$s = \frac{k}{k_s} ln\ \frac{r_s}{r_{wh}} - ln\ \frac{r_s}{r_w} \quad (10)$$

As long as the radius of wormhole penetration is greater than the radius of damage, Eq. (10) remains valid. Alternatively, if the well was initially undamaged or if the wormhole radius was higher than the original damage radius, the skin effect during acidification is assumed to be infinite, and the following Eq. (10) is used to represent this:

$$s = -ln\ \frac{r_{wh}}{r_w} \tag{11}$$

Eqs. (10) and (11), which assume that the injection rate is kept constant during the treatment for the damaged zone, are used to determine the skin impact expected by the volumetric model during the injection,

$$s = -\frac{k}{2k_s} ln\ \left[\left(\frac{r_w}{r_s}\right)^2 + \frac{V}{PV_{bt}\pi r_s^2 \phi h}\right] - ln\ \frac{r_s}{r_w} \tag{12}$$

furthermore, since wormholes that penetrate beyond the affected zone or there is no damage,

$$s = -\frac{1}{2} ln\ \left[1 + \frac{V}{PV_{bt}\pi r_s^2 \phi h}\right] \tag{13}$$

Both Buijse-Glasbergen and Furui models are used to calculate the radius of the wormhole region for discrete injection times. The skin factor is calculated using Eq. (10) or Eq. (11) for each r_{wh} obtained using these models.

3. Results and Discussion

According to the oil ministry's data release letter, we received a 1.34 m rock core section from the Mi4 unit, more precisely from the Mishrif formation. The Ahdeb field's operator, CNPC (Al-Waha), has previously drilled this core section and extracted plug samples with a diameter of 2.5 cm for the reservoir development plan. Therefore, only a limited number of specimens (11 plugs) were recovered from this core section with a 3.78-cm diameter and length variation (**Fig. 4**).

Figure 4. Extracted plug samples with a diameter of 2.5 cm from the core section**(Alameedy, 2022)**.

Choosing a reasonable flow rate of acid injection for each test is critical. There are three distinct flow zones: the compact dissolving, the wormholes, and the branching regions. A high acid injection rate produces the branching zone; a low acid injection rate produces the compact dissolving part, and a medium acid injection rate creates wormholes.

The maximum injection rate may be determined using Darcy's law. There is no backpressure (the outlet pressure will be 14.7 psi); hence, the greatest pressure dirop across the core is 3535.7 psi from the maximum 3550 psi pressure the syringe pump can supply. The greatest pressure drop is directly proportional to the maximum injection rate. The maximum flow rate may be determined using the core size, fluid viscosity, and rock permeability. To avoid damaging the syringe pump,

the flow irate of the experiment should be lower than the maximum flow rate necessary to stay within the limits of the high-pressure pump.

Eq. 2 claimed that (**Buijse** and **Glasbergen, 2005)** established a semiempirical model to estimate the breakthrough volume and wormhole propagation rate of pores. In this case, their model could match our collected data curve to find the optimal pore volume that generated the wormhole ($PV_{\mathrm{bt-opt.}}$) during the breakthrough and the corresponding optimal interstitial velocity ($v_{i-\mathrm{opt}}$). The **Eq. 2** can be slightly modified by replacing one variable y with 1/3 and equalizing with *f(Vi)* in the left hand side, yield **(Buijse** and **Glasbergen, 2005)**:

$$PV_{\mathrm{bt}} = PV_{\mathrm{bt-opt}} \left(\frac{v_i}{v_{i-\mathrm{opt}}}\right)^{1/3} \left\{1 - \exp\langle -4 \left(\frac{v_i}{v_{i-\mathrm{opt}}}\right)^2 \rangle\right\}^2 = f(V_i) \quad (14)$$

From the experiment, it is possible to determine the values of PV_{bt} and v_i straightforwardly. With the least squares approach, it is possible to fit the experimental data, which will also result in $PV_{\mathrm{bt-opt}}$ and v_{i-opt} being calculated.

$$J = \sum_i^n \left[PV_{bt}^i - f\left(v_i^i\right)\right]^2 \quad (15)$$

Where J is the difference between the observed and estimated pore volume values at breakthrough, and n denotes the number of data points from the experiment. The residue J should be kept to a bare minimum in order to get the best results. This may be accomplished by choosing the appropriate $PV_{\mathrm{bt-opt}}$ and $v_{i-\mathrm{opt}}$ parameters and applying **Eq. 14**. It is possible to rapidly and easily design the curve in an Excel sheet after the determination of $PV_{\mathrm{bt-opt}}$ and $v_{i-\mathrm{opt}}$. **Fig. 5** shows a fitting curve for a set of trials, including nine plug samples.

Because of experimental error, there may be some degree of ambiguity or faulty data points. Data like this will impact $PV_{\mathrm{bt-opt}}$ and $v_{i-\mathrm{opt}}$ curve fitting outcomes and values. The minimum value of J found 3.62 yields the $PV_{\mathrm{bt-opt}}$ is 2.73 and the $v_{i-\mathrm{opt}}$=0.6 cm/min.

As a result, it is recommended that the negative data points clearly out of line with the trend be removed. The curve may need to be recalculated.

Study after study has shown a certain minimum quantity of acid is necessary to propagate the core wormhole across a particular rock type, acid system, flow rate, and temperature **(Alameedy** and **Al-haleem, 2022; Fredd** and **Fogler, 1998; Wang et al., 1993)**. Comparing test results from cores

with different porosity and diameter is easier when interstitial velocity (vi) is used instead of acid injection rate (q).

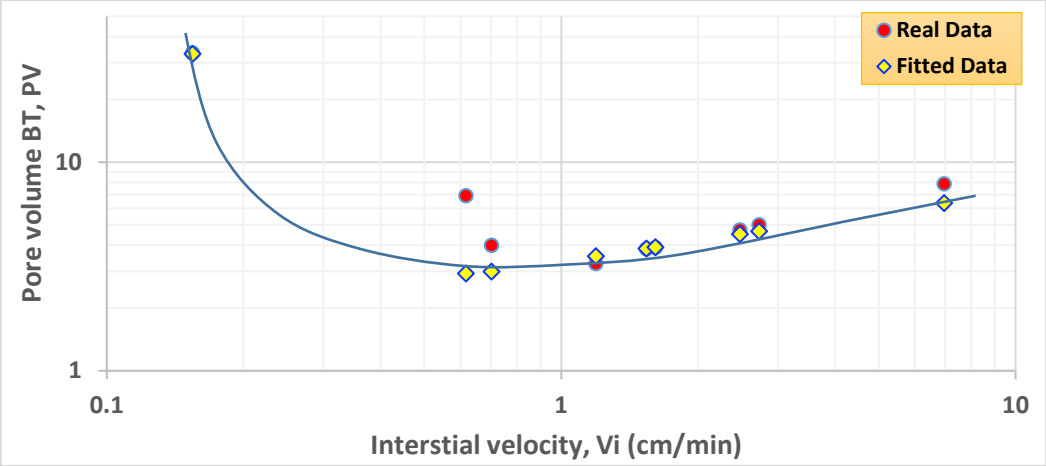

Figure 5. Picking the appropriate $\boldsymbol{PV_{bt-opt}}$ and $\boldsymbol{v_{i-opt}}$ parameters.

Fig. 6 shows the results of linear core flow testing for several parameter combinations (temperature, acid type, and rock). Our experimental data were redrawn using core samples collected from the Mi4 unit, while other data were gathered from the literature **(Buijse** and **Glasbergen, 2005; Fredd** and **Fogler, 1998).** Injection of HCl into limestone results in this distinctive wormholing effect. Similarities in the curvature of the curves are noteworthy. There are three unique zones, each defined by a different kind of dissolution: face dissolution (low velocity), wormhole dissolution (optimum rate), and uniform dissolution (high velocity):

1. If the injection rate or velocity is low enough, Hcl will quickly expand on the front of the plug sample, and no or only brief wormholes develop. Pore volume consumed is high at the time of breakthrough. Wormholes will not grow long enough to escape the damaged area during an acid treatment, so this must be avoided entirely.
2. When the acid injection rate is increased, wormholes begin to form because the acid can go deeper before spending all of its energy. The best injection rate is one that delivers just enough acid to the tip to allow for the growth of a single wormhole while preventing excessive side branching. The pore volume required for breakthrough is reduced to its lowest possible value when the optimal rate of $v_{i-\mathrm{opt}}$ is achieved ($PV_{\mathrm{bt-opt}}$).
3. While many wormholes may arise at the wormhole's tip due to a strong acid flow, the dissolving process is dominated by uniformity. A decrease in the pace of wormhole expansion will be the consequence of tip splitting and side branching. Even though large injection rates may still produce wormholes, the process is less effective than optimal injection rates.

Generally speaking, the amount of acid needed to propagate a wormhole grows slowly when the injection rate rises above the optimum. Still, the acid volume necessary to propagate a wormhole drops fast when the injection rate is below the optimum. This suggests that a higher injection rate is preferable to a lower one.

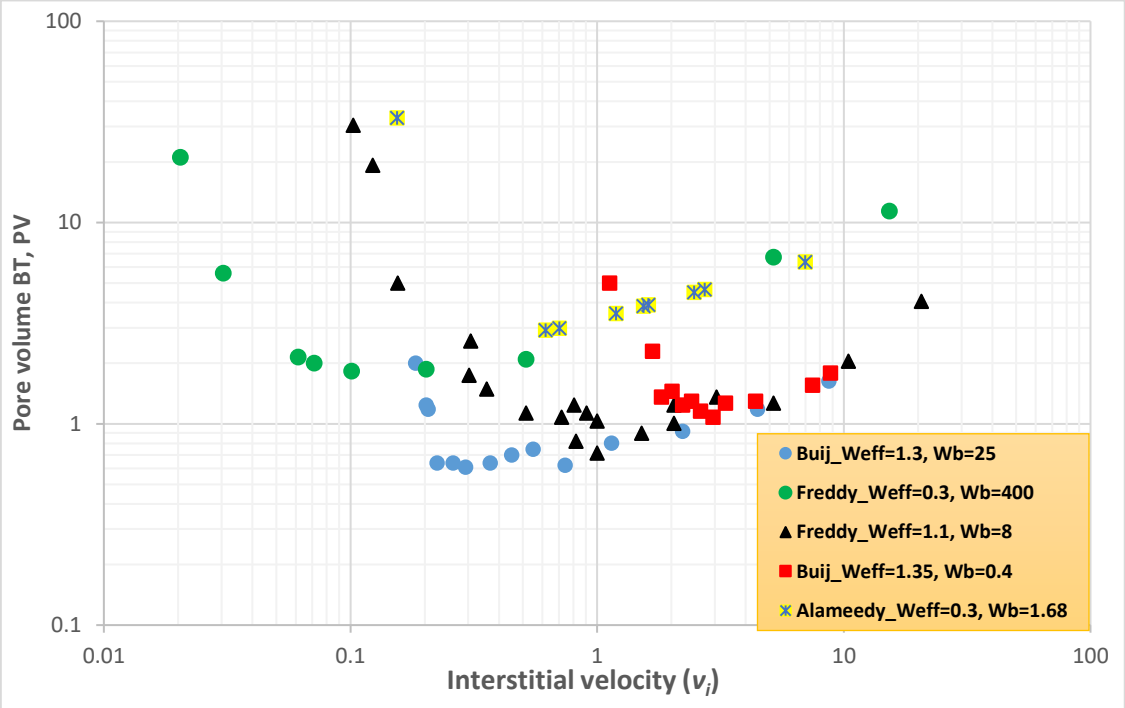

Figure 6. The findings of the acid flooding test PV_{bt} plotted as a function of the v_i. Data were obtained from **(Buijse** and **Glasbergen, 2005; Fredd** and **Fogler, 1998);** our data was created by modeling using **Eq. (14)**.

3.1.1 Upscaled Global Model for Wormhole Propagation

The global models described in Section 1.1 are the most valuable resources in designing and understanding acidizing treatments in carbonate rocks. Since these models are based on empirical evidence, they need data from actual lab experiments or observations in the field, depending on the acid system (**Table 1**). Wormhole propagation around a wellbore may be predicted using the most prevalent models for upscaling our laboratory research. With such broad channels, it is often thought that the pressure loss across the wormhole area in carbonates is low, such that increasing the well's skin effect is equivalent to creating new wormholes there. Due to this reason, wormhole propagation models may be used to forecast how carbonate skin would evolve under the acidic treatment of the matrix.

Table 1. All the required data from actual lab experiments and observations in the field for well Ad-12.

r_w **(ft)**	0.328	$PV_{bt,opt}$	2.75	$r_{wh,rep1}$ **(ft)**	3
φ	0.15	$v_{ibt,opt}$ **(cm/min)**	0.6	$r_{wh,rep2}$ **(ft)**	1
h (ft)	45	d_{core} **(in)**	1.5	f_1	0.143

q (bpm)	2.5	ε_1	0.53	f_2	0.14
k (md)	15	ε_2	0.63	α_z	0.35
k_s ***(md)***	1.5	L_{rep1}	1	m_{wh}	12.57
r_s ***(ft)***	0.828	L_{rep2}	1	N_{AcF}	0.0146
β_f	0.21	ρ_{matrix} **(gm/cc)**	2.71	ρ_{acid} **(gm/cc)**	1.07
C0HCL	1	de_{wh} **(ft)**	0.00183	Gel Acid	HCl%15

The linear flow core flooding acidification experiment was incorporated into the wellbore upscaling using the four models described in Section 2.1. At the pore scale, it's found the $PV_{\mathrm{bt-opt}}$ value to be 2.73 and the $v_{i-\mathrm{opt}}$value to be 0.6 cm/min from **Fig. 5**, while the remaining data in **Table 1** were obtained from real field reports and acid stimulation job data sheets. There is a comparison of r_{wh} and time in **Fig. 6**, including all global models. Both the volumetric model introduced by **(Economides** and **Nolte, 2000)** and **(Buijse** and **Glasbergen, 2005)** model imply less wormhole penetration than the upscaled models **(Schwalbert et al., 2017)** model and the **(Furui et al., 2012)** model in **Fig. 7**. The volumetric model does not reflect the sensitivity of PV_{bt} on acid flow, when injection time rises, the underestimating of wormhole propagation in the non-upscaled models becomes worse. Depending on the interstitial velocity at the radial distance to which the wormholes have spread in the Buijse-Glasbergen model, the wormhole velocity varies (r_{wh}). According to Furui et al., their model can accurately estimate the analogous wormhole diameter (d_{ewh}) of comparable wormholes as long as the value employed is acceptable. The Schwalbert model is more realistic than other models because it considers the varying wormhole outcomes achieved at different sizes, and it utilizes the data collected using cores of any size as input. Furthermore, it is used to verify its usefulness in reproducing core flooding studies and at a greater scale near field settings and to mimic situations that have not yet been tested, such as the effects of the scale in wormhole propagation and anisotropic formations.

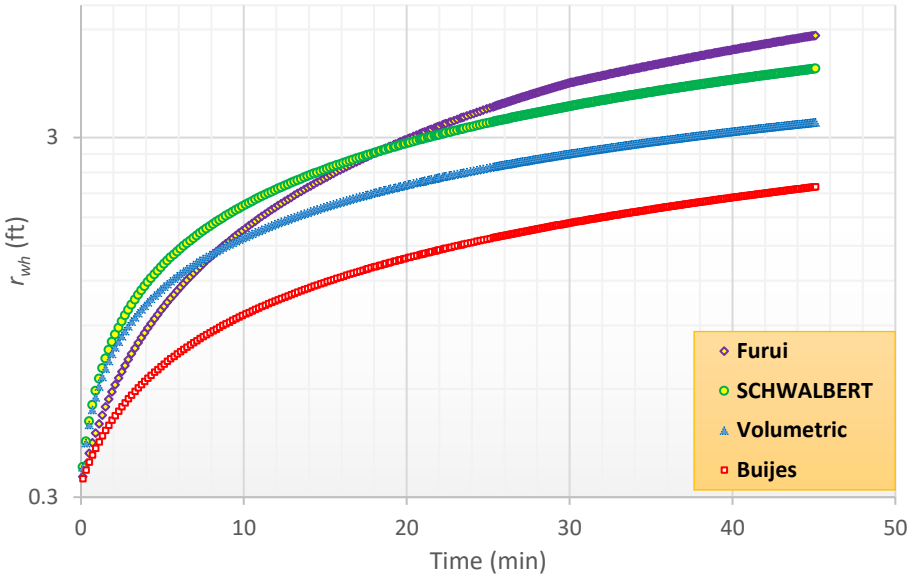

Figure Error! No text of specified style in document.**7.** Application of wormhole propagation global models to calculate the wormhole radius versus time for well Ad-12.

As shown by the models provided, a prediction of wormhole propagation depth into the formation using the pore volumes required to break through a rock/acid system. Carbonate rocks with a high degree of heterogeneity, including naturally vuggy limestones or fractured, have a lower value for this characteristic than more homogenous rocks.

3.1.2 Monitoring how well the acidizing treatment performance.

When calculating and displaying the skin factor as a function of injection time using the wormhole propagation findings from **Fig. 7**, further assuming the formation has a permeability of 15 md and a damaged zone with a permeability of 5 md extending 0.5 ft into the formation. By calculating **Eqs**. 10 to 13 in the manner outlined in Section 1.2, if the radius of total damage (rs) penetrates 0.828 feet into the formation, **Eq. 12** is used to compute the skin for the volumetric model, while **Eq. 10** is used for the other models. Beyond the affected zone (distance of more than 0.828 ft), the skin factor calculated versus time using **Eq. 13** for the volumetric model and equation 3.18 for the rest models. The Schwalbert, Furui, and Buiji Models are used to take a series of time steps and compute the radius of wormhole propagation from **Fig. 7** at each discrete injection time. All estimates of skin factor for these models are shown in **Fig. 8**; the acid injection rate in well Ad-12 was 2.5 bpm based on the acid treatment report. As long as less than 1.88 gal/ft of acid is used to stimulate this damaged well, wormholes may be propagated across the damaged zone. As wormholes move deeper into the formation due to the continued acid injection, the skin factor is expected to decrease with time. Injecting at a greater pace might result in a more potent deep stimulation.

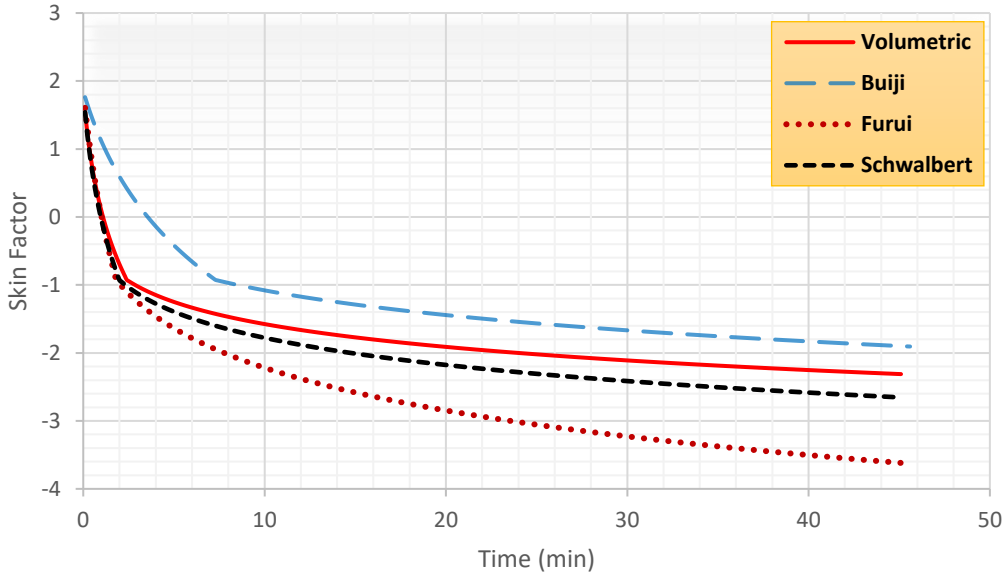

Figure 8. Application of wormhole propagation global models to calculate the skin factor versus time for Well Ad-12.

The recorded data for the stimulated wells are taken from the build-up test reports and shown in **Table 2**. The models indicated underestimated values, which may be attributed to the models' inability to account for transient radial flow pressure analysis, well completion and heat transfer modeling through real-time treatment. Evidently, Ad-12 build-up analysis yields a skin value of -3.97, which is about comparable to the skin values of the other models but is closer to the Shwalbert model.

Table 2. Field reported data for the stimulated wells claimed from the build-up test.

Well	k (md)	φ	Skin	Date of Test
Ad 2-3	62.54	19.43	-4.75	03/2012
Ad 2-3	13.00	19.43	-3.75	06/2012
Ad 4-1	5.36	19.48	-3.54	10/2012
Ad-12	15.04	19.1	-3.97	12/2011
Ad 5-11H	7.63	21.12	-7.52	03/2016
Ad 0-3H	11.84	20.85	-7.69	09/2018
Ad 3-5	25.94	19.54	-5.66	03/2020

4. CONCLUSIONS

1. Significant challenges are encountered during acid stimulation operations in the Mishrif reservoir of the Ahdeb oil field, including high injection pressures, with several acid treatment failures recorded. The significant failure rate of oil well stimulation in this deposit necessitates more research. Thus experimental investigations of the effect of

acidizing on the geomechanical properties of the Mi4 formation of the Mishrif reservoir were presented. Several acid-flooding experiments were performed on different rock samples to study the influence of mineralogy and confirm the outcomes' consistency.

2. The propagation of acid-induced wormhole and its effect on rock strength were analyzed and compared to intact rocks.
3. The acid efficiency curve yielded the lowest pore volume injected at the breakthrough of the $PV_{\mathrm{bt-opt}}$ is 2.73 and the $v_{i-\mathrm{opt}}$=0.6 cm/min; thus, the optimum injection rate that results in an optimal possible wormhole and the least quantity of acid being used for this reservoir is 2.16 cc/min.
4. The estimated oil gain volume and percentage for the Mi4 unit in Ad-12 using skin value, particularly -3.97 computed from Stimpro software for real stimulation acid job, it is yield enhancement in production of oil gain volume 6154 barrels as well as 105% increase of gain percentage for three months after matrix acidizing.
5. In acid flooding, rock weakening does not necessarily mean deterioration/sand production/instability; it depends on other factors. For instance, it could be due to acid-induced fracture/wormhole, which corresponds to porosity enhancement that resulted in lower acoustic readings and, thus, reduced rock competence. Therefore, it is recommended that independent investigations of the bulk rock and fractured surface strength be conducted to make a clear distinction between these occurrences. Further, following the experimental results (acid stimulation) presented in this study for the Mi4 formation of the Mishrif reservoir pre- and post-acid treatment, it showed that despite the observed rock's mechanical properties alterations observed which show wormhole propagation, effective wormholes/flow paths were created for hydrocarbon flow from the reservoir into the wellbore. The results presented implied a successful acid treatment of the Ahdeb oilfield despite the development problems of the Ahdeb oilfield reported during the stimulation operation of this reservoir formation.

NOMENCLATURE

d_{core} = Core diameter
d_{s1} = Scale related to the decrease in PVbt, opt
d_{s2} = Scale related to the decrease in vi, opt
h = Reservoir thickness, net pay
J = productivity or injectivity index
k = Permeability (scalar)
L = Wellbore length
l_{perf} = Perforation length
l_{wh} = Wormhole length in a linear geometry
NAC = Acid capacity number
PV_{bt} = pore volumes to breakthrough, in wormhole propagation
q = Flow rate (injection or production rate)

r_w = wellbore radius
r_{wh} = Radius of cylindrical wormholed region
$PV_{bt,\ opt}$ in radial geometry
$v_{i,\ opt}$ in radial geometry
s = Skin factor
T = Temperature
t = Time
v_i = Interstitial velocity
$v_{i,\ opt}$ = Optimal interstitial velocity, in wormhole propagation

REFERENCES

Al-Hashmi, L., Qutob, H., and El-Halfawi, S., 2010. Successful Well Stimulation Projects Boost Production from Iraq's South Oil Fields, *SPE European Formation Damage Conference, The Hague, Netherlands*, https://doi.org/10.2118/138726-MS

Al-Waha Pet. Corp. Ltd., 2010. *AD-012, FINAL GEOLOGICAL REPORT, AHDEB OILFIELD, IRAQ*.

Al-Yaseri, A. Z., Sattam, M., and Alameedy, U., 2013. Improve Permeability Prediction for One of Iraqi Carbonate Oil Reservoir, *Journal of the University of Babylon*, *21*(February), 1289–1300.

Alameedy, U., 2012. Permeability Evaluation of Zubair Formation Using Well Logs, *GEO 2012*, cp-287-00002, https://doi.org/https://doi.org/10.3997/2214-4609-pdb.287.1117261

Alameedy, U., 2022. *Experimental study of matrix acidization for Mishrif Formation/Ahdeb oil field*, https://doi.org/10.13140/RG.2.2.25412.91525

Alameedy, U., and Al-haleem, A., 2022. The Impact of Matrix Acidizing on the Petrophysical Properties of the Mishrif Formation: Experimental Investigation, *Iraqi Geological Journal*, *55*(1E), 41–53, https://doi.org/10.46717/igj.55.1E.4Ms-2022-05-20

Alameedy, U., Alhaleem, A. A., Isah, A., Al-Yaseri, A., Mahmoud, M., and Salih, I. S., 2022. Effect of acid treatment on the geomechanical properties of rocks: an experimental investigation in Ahdeb oil field, *Journal of Petroleum Exploration and Production Technology*, https://doi.org/10.1007/s13202-022-01533-x.

Azeez, H. S., Al-Dabaj, D. A. A., and Lazim, D. S., 2020. Petrophysical Analysis of an Iraqi Gas Field (Mansuriya Gas Field), *Journal of Engineering*, *26*(3), 100–116. https://doi.org/10.31026/j.eng.2020.03.09

Bagrintseva, K. I., 2015. *Carbonate Reservoir Rocks*, John Wiley & Sons, Inc. https://doi.org/10.1002/9781119084006

Buijse, M., and Glasbergen, G., 2005. A Semi-Empirical Model To Calculate Wormhole Growth in Carbonate Acidizing, *SPE Annual Technical Conference and Exhibition, Dallas, Texas*, https://doi.org/10.2118/96892-MS

Daccord, G., and Lenormand, R., 1987. Fractal patterns from chemical dissolution, *Nature*, *325*(6099), 41–43, https://doi.org/10.1038/325041a0

Daccord, G., Touboul, E., and Lenormand, R., 1989. Carbonate Acidizing: Toward a Quantitative Model of the Wormholing Phenomenon, *SPE Production Engineering*, *4*(01), 63–68, https://doi.org/10.2118/16887-PA

Doerler, N., and Prouvost, L. P., 1987. Diverting Agents: Laboratory Study and Modeling of Resultant Zone Injectivities, *SPE 16250*.

Dong, K., Zhu, D., and Hill, A. D., 2017. Theoretical and experimental study on optimal injection rates in carbonate acidizing, *SPE Journal*, *22*(3), 892–901, https://doi.org/10.2118/178961-pa

Economides, M. J., Hill, A. D., and Ehlig-and Economides, C., 1994. *Petroleum Production Systems*.

Economides, M. J., Hill, A. D., Ehlig-and Economides, C., and Zhu, D., 2013. *Petroleum Production Systems* (2nd Edition), PENTICE HALL.

Economides, M. J., and Nolte, K. G., 2000. *Rerservoir Stimulation* (M. J. Economides and K. G. Nolte (eds.); 3rd ed., Wiley.

Fredd, C. N., and Fogler, H. S., 1996. Alternative Stimulation Fluids and Their Impact on Carbonate Acidizing, *SPE Formation Damage Control Symposium, Lafayette, Louisiana*, https://doi.org/10.2118/31074-MS

Fredd, C. N., and Fogler, H. S., 1998. Alternative Stimulation Fluids and Their Impact on Carbonate Acidizing, *SPE Journal*, *3*(01), 34–41, https://doi.org/10.2118/31074-PA

Furui, K. ., Burton, R. C., Burkhead, D. W., Abdelmalek, N. A., Hill, A. D., Zhu, D., and Nozaki, M., 2012a. A Comprehensive Model of High-Rate Matrix-Acid Stimulation for Long Horizontal Wells in Carbonate Reservoirs: Part I—Scaling Up Core-Level Acid Wormholing to Field Treatments, *SPE Journal*, *17*(01), 271–279, https://doi.org/10.2118/134265-PA

Furui, K., Burton, R. C., Burkhead, D. W., Abdelmalek, N. A., Hill, A. D., Zhu, D., and Nozaki, M., 2012b. A Comprehensive Model of High-Rate Matrix-Acid Stimulation for Long Horizontal Wells in Carbonate Reservoirs: Part I—Scaling Up Core-Level Acid Wormholing to Field Treatments, *SPE Journal*, *17*(01), 271–279, https://doi.org/10.2118/134265-PA

Furui, K., Burton, R. C., Burkhead, D. W., Abdelmalek, N. A., Hill, A. D., Zhu, D., and Nozaki, M., 2012c. A comprehensive model of high-rate matrix-acid stimulation for long horizontal wells in carbonate reservoirs: Part II-wellbore/reservoir coupled-flow modeling and field application, *SPE Journal*, *17*(1), 280–291, https://doi.org/10.2118/155497-PA

Furui, K., Zhu, D., and Hill, A. D., 2003. A Rigorous Formation Damage Skin Factor and Reservoir Inflow Model for a Horizontal Well, *SPE Production & Facilities*, *18*(03), 151–157, https://doi.org/10.2118/84964-PA

Gong, M., and El-Rabaa, A. M., 1999. Quantitative Model of Wormholing Process in

Carbonate Acidizing, *SPE Mid-Continent Operations Symposium, Oklahoma City, Oklahoma*, https://doi.org/10.2118/52165-MS

Hill, A. D., and Galloway, P. J., 1984. Laboratory and Theoretical Modeling of Diverting Agent Behavior, *JPT*, 1157–1163.

Huang, T., Zhu, D., and Hill, A. D., 1999. Prediction of Wormhole Population Density in Carbonate Matrix Acidizing, *SPE European Formation Damage Conference, The Hague, Netherlands*, https://doi.org/10.2118/54723-MS

Lucia, F. J., 2007. *Carbonate Reservoir Characterization*, Springer Berlin Heidelberg, https://doi.org/10.1007/978-3-540-72742-2

Mahmoud, M. A., Nasr-El-Din, H. A., De Wolf, C. A., and LePage, J. N., 2011. Optimum Injection Rate of A New Chelate That Can Be Used To Stimulate Carbonate Reservoirs, *SPE Journal*, *16*(04), 968–980, https://doi.org/10.2118/133497-PA

McDuff, D. R., Shuchart, C. E., Jackson, S. K., Postl, D., and Brown, J. S., 2010. Understanding wormholes in carbonates: Unprecedented experimental scale and 3-D visualization, *Proceedings - SPE Annual Technical Conference and Exhibition*, *3*, 2321–2329, https://doi.org/10.2118/134379-ms

Neeamy, A. K., and Selman, N. S., 2020. Building 1D Mechanical Earth Model for Zubair Oilfield in Iraq, *Journal of Engineering*, *26*(5), 47–63, https://doi.org/10.31026/j.eng.2020.05.04

Noori, A. K., Lazim, S. A., and Ramadhan, A. A., 2019. Geological Model of the Tight Reservoir (Sadi Reservoir-Southern of Iraq), *Journal of Engineering*, *25*(6), 30–43, https://doi.org/10.31026/j.eng.2019.06.03

Schechter, R. S., and Gidley, J. L., 1969. The change in pore size distribution from surface reactions in porous media, *AIChE Journal*, *15*(3), 339–350, https://doi.org/10.1002/aic.690150309

Schwalbert, M. P., Zhu, D., and Daniel Hill, A., 2017. Extension of an empirical wormhole model for carbonate matrix acidizing through two-scale continuum 3D simulations, *Society of Petroleum Engineers - SPE Europec Featured at 79th EAGE Conference and Exhibition*, 73–95, https://doi.org/10.2118/185788-ms

Taha, R., Hill, A. D., and Sepehrnoori, K., 1989. Sandstone Acidizing Design Using a Generalized Model, *SPE Production Engineering*, *4*, 49–55.

Talbot, M. S., and Gdanski, R. D., 2008. Beyond the Damkohler Number: A New Interpretation of Carbonate Wormholing, *Europec/EAGE Conference and Exhibition, Rome, Italy*, https://doi.org/10.2118/113042-MS

Tardy, P. M. J., Lecerf, B., and Christanti, Y., 2007. An Experimentally Validated Wormhole Model for Self-Diverting and Conventional Acids in Carbonate Rocks under Radial Flow Conditions, *European Formation Damage Conference, Scheveningen, The Netherlands*, https://doi.org/10.2118/107854-MS

Wang, Y., Hill, A. D., and Schechter, R. S., 1993. The Optimum Injection Rate for Matrix Acidizing of Carbonate Formations, In *SPE Annual Technical Conference and Exhibition* (p. SPE-26578-MS), https://doi.org/10.2118/26578-MS

Widarsono, B., Jaya, I., and Muladi, A., 2006. Permeability Vertical-to-horizontal Anisotropy In Indonesian Oil and Gas Reservoirs: A General Review, *The International Oil Conference and Exhibition in Mexico, Cancun, Mexico*, https://doi.org/10.2118/103315-MS